Xin *et al. Radiation Oncology* (2024) 19:114
https://doi.org/10.1186/s13014-024-02508-4

Radiation Oncology

RESEARCH Open Access

Dose tracking assessment for magnetic resonance guided adaptive radiotherapy of rectal cancers

Xin Xin[1,2], Bin Tang[2*], Fan Wu[2], Jinyi Lang[2], Jie Li[2], Xianliang Wang[2], Min Liu[2], Qingxian Zhang[1], Xiongfei Liao[2], Feng Yang[1,2] and Lucia Clara Orlandini[2]

Abstract

Background Magnetic resonance-guided adaptive radiotherapy (MRgART) at MR-Linac allows for plan optimisation on the MR-based synthetic CT (sCT) images, adjusting the target and organs at risk according to the patient's daily anatomy. Conversely, conventional linac image-guided radiotherapy (IGRT) involves rigid realignment of regions of interest to the daily anatomy, followed by the delivery of the reference computed tomography (CT) plan. This study aims to evaluate the effectiveness of MRgART versus IGRT for rectal cancer patients undergoing short-course radiotherapy, while also assessing the dose accumulation process to support the findings and determine its usefulness in enhancing treatment accuracy.

Methods Nineteen rectal cancer patients treated with a 1.5 Tesla MR-Linac with a prescription dose of 25 Gy (5 Gy x 5) and undergoing daily adapted radiotherapy by plan optimization based on online MR-based sCT images, were included in this retrospective study. For each adapted plan ($\mathrm{TP}_{\mathrm{adap}}$), a second plan ($\mathrm{TP}_{\mathrm{IGRT}}$) was generated by recalculating the reference CT plan on the daily MR-based sCT images after rigid registration with the reference CT images to simulate the IGRT workflow. Dosimetry of $\mathrm{TP}_{\mathrm{adap}}$ and $\mathrm{TP}_{\mathrm{IGRT}}$ was compared for each fraction. Cumulative doses on the first and last fractions were evaluated for both workflows. The dosimetry per single fraction and the cumulative doses were compared using dose-volume histogram parameters.

Results Ninety-five fractions delivered with MRgART were compared to corresponding simulated IGRT fractions. All MRgART fractions fulfilled the target clinical requirements. IGRT treatments did not meet the expected target coverage for 63 out of 94 fractions (67.0%), with 13 fractions showing a V95 median point percentage decrease of 2.78% (range, 1.65-4.16%), and 55 fractions exceeding the V107% threshold with a median value of 15.4 cc (range, 6.0-43.8 cc). For the bladder, the median $\mathrm{D}_{15\mathrm{cc}}$ values were 18.18 Gy for the adaptive fractions and 19.60 Gy for the IGRT fractions. Similarly the median $\mathrm{D}_{5\mathrm{cc}}$ values for the small bowel were 23.40 Gy and 25.69 Gy, respectively. No statistically significant differences were observed in the doses accumulated on the first or last fraction for the adaptive workflow, with results consistent with the single adaptive fractions. In contrast, accumulated doses in the IGRT workflow showed significant variations mitigating the high dose constraint, nevertheless, more than half of the patients still did not meet clinical requirements.

*Correspondence:
Bin Tang
jackytang86@163.com

Full list of author information is available at the end of the article

Conclusions MRgART for short-course rectal cancer treatments ensures that the dose delivered matches each fraction of the planned dose and the results are confirmed by the dose accumulation process, which therefore seems redundant. In contrast, IGRT may lead to target dose discrepancies and non-compliance with organs at risk constraints and dose accumulation can still highlight notable dosimetric differences.

Keywords Adaptive radiotherapy, MR-linac, Dose tracking, Synthetic CT, Rectal cancer; Dose accumulation

Background

The estimated incidence of new cases of colon rectal cancer (CRC) in the USA in 2024 is 152,810, according to the American Cancer Society Radiotherapy, with 46,220 of these cases being rectal cancer [1]; CRC is the second leading cause of all cancer-related deaths in the United States and between the top five leading causes of cancers death in China, which recorded 240 000 deaths in 2022 [2].

Radiotherapy is a successful treatment option for individuals with rectal cancer [3]; when combined with chemotherapy, neoadjuvant radiotherapy, which involves prescribing around 50 Gy in fractions of 1.8–2.0 Gy (referred to as long-course radiotherapy), is widely accepted as the standard treatment for locally advanced rectal cancers. For non-locally advanced stage III rectal cancer, short-course radiotherapy (SCRT), consisting of neoadjuvant therapy (5.0 Gy x 5 fractions)) is a valid option. Both these approaches are typically followed by total mesorectal excision (TME) surgery [4–6].

For radiotherapy treatment planning, the superior soft-tissue contrast in magnetic resonance imaging (MRI) compared to computed tomography (CT) images [7] provides excellent visualization of both the tumor target and organs at risk, improving the simulation and treatment technique [8, 9]. This enables the safer delivery of higher doses to the target and better sparing of organs at risk (OARs), namely the rectum and bladder. However, the modifications or displacements of target volumes and OARs, relative to the radiation beam frequently occur because of patient positioning and different filling and pressure effects from OARs [10]; these can result in significant dosimetric changes because of the sharp dose gradients between the target and normal tissue. Unfortunately, such anatomical modifications may cause underdosing of target organs and/or over-dosing of OARs.

Image-guided radiotherapy (IGRT) is commonly used to reduce setup errors in patient positioning and in the inter-fraction organ motion [11]. Typically, the correction parameter involves moving the treatment table to re-position the shifted target point to the isocenter of the treatment device. Target-point correction is a commonly used approach in IGRT and has shown to be particularly effective for treating tumor sites with minimal deformations. Despite its benefits, this method does not address anatomical changes like volume fluctuations in OARs or variations in the planning target volume (PTV) that may occur throughout treatment. Previous researches have discussed the potential of adaptive radiotherapy in addressing inter-fraction motion and has suggested offline strategies that rely on geometric and dosimetric feedback [12].

Recently, adaptive radiotherapy has benefited from magnetic resonance linear accelerators (MR-Linacs), which integrate an MRI scanner [13]. Adaptive radiotherapy guided by MRI images is more effective for treatments where soft tissue visualisation is crucial and allows online adaptation of dose distribution to daily anatomy [14]. This dual advantage – superior soft tissue imaging compared to cone beam CT and real-time anatomical contour adaptation- makes this technology unique, explaining the significant interest and ongoing researches. Consequently, daily online adaptation in magnetic resonance-guided adaptive radiotherapy (MRgART) effectively handles interfraction anatomical variations, previously considered major approximations [15].

Dose accumulation may be used to better estimate the total dose delivered to the patient at some time points of the treatment; advanced accumulation strategies to sum the doses from individual plans may account for the anatomical changes; typically they involve deformable image registration between planning images, or deformable dose mapping, and voxel-wise dose summation [16, 17].

We investigated how inter-fractional variations in patient anatomy affected the difference between planned and delivered doses in rectal cancer patients undergoing an IGRT or MRgART treatment. A detailed analysis was performed among the single fractions. Moreover, the dose cumulated at the end of the SCRT treatment was evaluated for each patient, on the first and last fraction, and for both MRgART and IGRT workflows.

Methods

Patient selection and MRgART workflow

Nineteen patients with rectal cancer undergoing a short course (25 Gy, 5 Gy x 5) with MRgART at 1.5 Tesla Unity MR-Linac (Unity, Elekta AB, Stockholm Sweden) were included in this retrospective study. The study was approved by the Ethics Committee of our Hospital (SCCHEC-02-2022-003).

CT simulation images were acquired with patients in the supine position using indexed positioning aids and KneeSTEP and FeetSTEP supports (IT-V, Innsbruck,

Table 1 Organs at risk constraints and planning target volume (PTV) goals for a short course of radiotherapy (25 gy, 5 gy x 5 fractions) for rectal treatment

Organ	Dose (Gy)	Volume
PTV	23.75 (95%D_{pre}^^)	> 99%
	26.75 (107% D_{pre}^^)	< 2 cc; ^< 5 cc
	27.50 (110% D_{pre}^^)	< 0.5 cc
Bladder wall	< 18.3	15 cc
	< 30	< 0.015 cc
Small Bowel	< 25	5 cc; *10 cc
Femoral Head	< 30	10 cc

^for the online adaptive plan; *optimal value; ^^prescription dose

Austria). T2-weighted magnetic resonance (MR) images were acquired in the same position, immediately after the CT scan; a Brilliance big bore scanner (Philips, Eindhoven, The Netherlands) and the Unity MR-Linac scanner were used for the CT and MR simulation, respectively. A bladder catheter was used both at simulations and at each treatment fraction to ensure consistent filling [10]. CT and MR images were exported into commercial software (MIM Software Inc, Cleveland Ohio, USA); after rigid registration of the simulation CT and MR images, experienced radiation oncologists delineated the target and OARs. The gross target volume, the mesorectal and the elective lymph nodes region's clinical target volumes, and the OARs were delineated following international guidelines [18]. PTV margins were created for the mesorectum with 5 mm in all directions. The treatment plans were performed in Monaco V-5.4 TPS, using ten to twelve individual beam angles and a 2 mm dose grid for the calculation; plans were optimised to achieve the clinical goals, particularly to encompass at least 99% the PTV with a dose of 23.75 Gy (corresponding to 95% of the dose prescribed) and limiting as much as possible doses to OARs following international guidelines and consensus [14, 19–22]. The details of the target dosimetric criteria and OAR constraints used for plan optimisation are reported in Table 1.

During the online session, MRI images were acquired and, after a rigid registration with the reference images, the contours were modified to match the patient's daily anatomy using a deformable registration. They were then manually adjusted and approved by the radiation oncologist. The daily adapted plan (TP_{adap}) was then optimised to meet the target goal and OARs constraints. The reference CT plan contains all the density bulk assignment information to be used on the online adaptive step where the adaptive plan calculation is performed using the MRI-based synthetic CT (sCT) [23, 24]. The information includes for each contour, its average electronic density

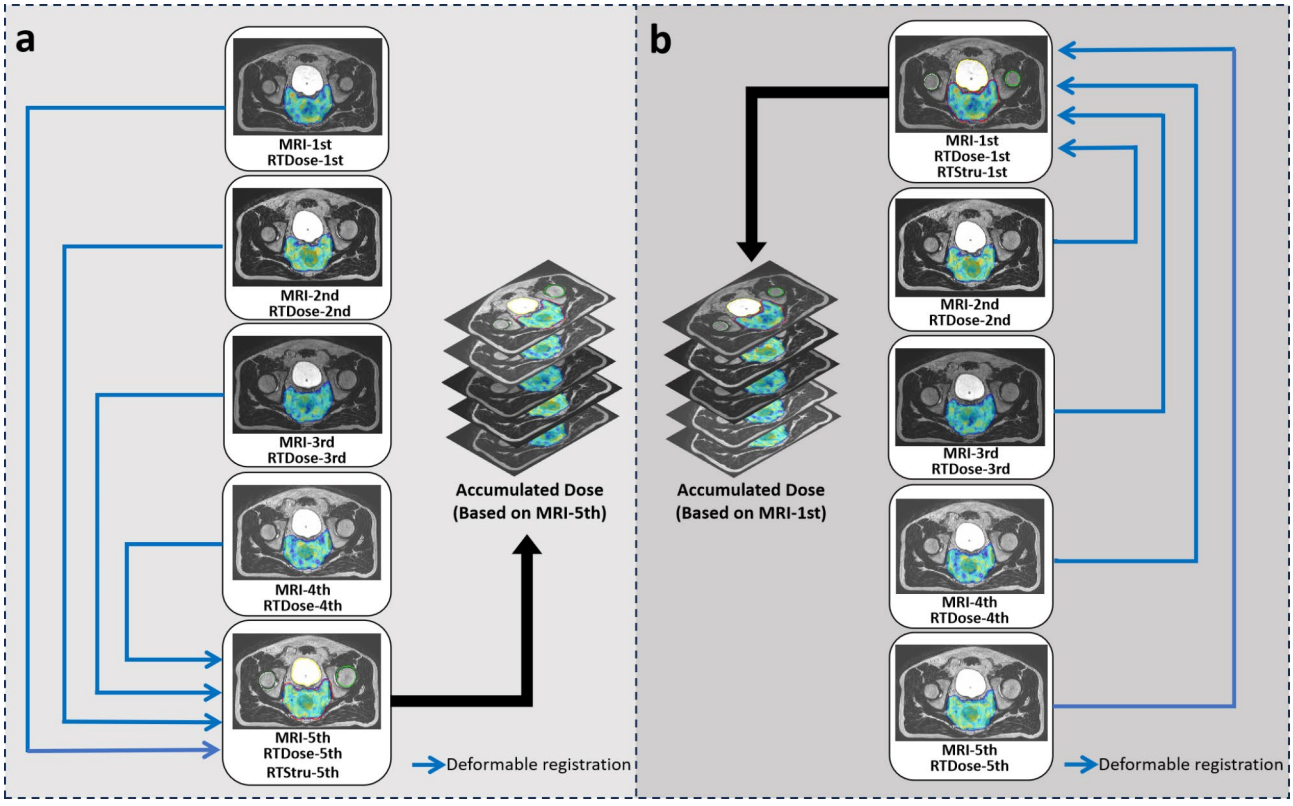

Fig. 1 Dose accumulation workflow, on the first (**a**) and last (**b**) fraction

Table 2 Dosimetric parameters for the target and organs at risk over 95 investigated fractions from TP_{adap} and TP_{IGRT} plans. Median values are shown, with the range in parenthesis. Significant differences ($p < 0.05$) are indicated in bold

	TP_{ADAP}	TP_{IGRT}	*p*
PTV $V_{23.75}$ (%)	99.59 (98.88–99.85)	99.23 (95.28–100.00)	< **0.001**
PTV $V_{26.75}$ (cc)	1.71 (0.00-5.95)	7.9 (0.04–43.80)	< **0.001**
Bladder D_{15cc} (Gy)	18.18 (13.07–23.32)	19.60 (15.07–24.37)	< **0.001**
Small Bowel D_{5cc} (Gy)	23.40 (13.88–24.80)	25.69 (14.05–26.43)	< **0.001**

(ED), and ED assignment priority in the case of overlapping contours.

Treatment plan of the simulated IGRT workflow

In IGRT treatments, reference CT images used for the reference plan are rigidly registered to the daily acquired images. Following this alignment, the patient's isocenter is moved to the registered position for treatment delivery. To assess the dose delivered during the IGRT workflow, a second treatment plan (TP_{IGRT}) was created for each adaptive session. This process entails recalculating the CT reference treatment plan on synthetic sCT images, which are derived from the daily online MRI after the daily registration; the original planning parameters remain unchanged during this recalculation.

Dose accumulation

To assess the accumulated dose at the end of the SCRT, for each fraction the daily MRI images, the updated structures matching the daily anatomy and the dose distribution were transferred into MIM workstation for processing. The dose delivered at each fraction with TP_{adap} and the dose recalculated at each fraction with TP_{IGRT} were accumulated on both the first and last fractions to estimate a potential range within which the actual dose might lie. In each dose accumulation process, transformation matrices were obtained by first performing rigid registration followed by deformable image registration (DIR) between the reference image (MRI-1st or MRI-5th) and the sequential daily online MRIs [25]. These transformation matrices were then applied to the dose distributions on each daily MRI to generate the deformed dose map. Finally, the deformed dose maps from the five fractions were summed up to yield the final cumulative dose. The workflow used in the accumulation process is shown in Fig. 1.

IGRT and MRgART workflow comparison

For each fraction, the dose delivered with TP_{IGRT} and TP_{adap} was compared. Target and OARs DVH dosimetric differences were assessed. Particularly for the target the volume receiving the prescribed dose (V_{Dpre}), and the maximum volume receiving 107% and 110% of the V_{Dpre} ($V_{26.75}$ and $V_{27.50}$, respectively); while for the OARs the dose received by 0.015, 5, 10, and 15 cc (($D_{0.015}$, D_{5cc}, D_{10cc}, D_{15cc}, respectively) were considered.

Results

A total of 95 fractions delivered with TP_{adap} on the daily MRI images were compared to the corresponding fractions recalculated with the TP_{IGRT} plan. Significant differences ($p < 0.01$) were observed for the target $V_{23.75}$ and $V_{26.75}$, bladder D_{15cc}, and small bowel D_{5cc} as reported in Table 2. Specifically, for 63 out of 95 fractions (66.3%), calculated with TP_{IGRT}, 55 fractions had $V_{26.75}$ values exceeding the constraints, with a median value of 14.57 cc (range, 6.03–43.79 cc). For 13 fractions, the

Table 3 Dose accumulated on the first and last fraction for MRgART and IGRT workflows; the results for representative DVH dosimetric parameters are reported as median values and range in parenthesis. ^ in bold significant differences ($p < 0.05$)

	[a]Acc fr	[b]MRgART	[c]IGRT	*p*
[d]PTV $V_{23.75}$ (%)	First	99.16 (93.33–99.84)	99.33 (98.05–99.69)	0.285
	Last	99.20 (98.68–99.67)	98.87 (97.07–99.31)	**0.000**
	p	0.976	**0.000**	
PTV $V_{26.75}$ (cc)	First	0.0 (0.0–0.0)	2.70 (0.00-36.91)	0.183
	Last	0.0 (0.0–0.0)	0.31 (1.42–7.48)	**0.022**
	p	0.163	**0.028**	
Bladder D_{15cc} (Gy)	First	18.92 (15.31–23.05)	19.54 (16.61–23.85	**0.034**
	Last	17.24 (13.37–22.18)	18.59 (13.28–22.94)	**0.009**
	p	0.155	**0.009**	
Small Bowel D_{5cc} (Gy)	First	23.05 (13.88–26.25)	23.34 (14.05–26.46)	**0.010**
	Last	25.98 (22.36–26.03)	25.56 (22.45–26.06)	**0.003**
	p	0.342	**0.009**	

[a] Fraction on which the dose has been accumulated

[b, c] Indicate the workflow followed: Magnetic Resonance Guided Radiotherapy and Image-guided radiotherapy, respectively

[d] Planning Target Volume

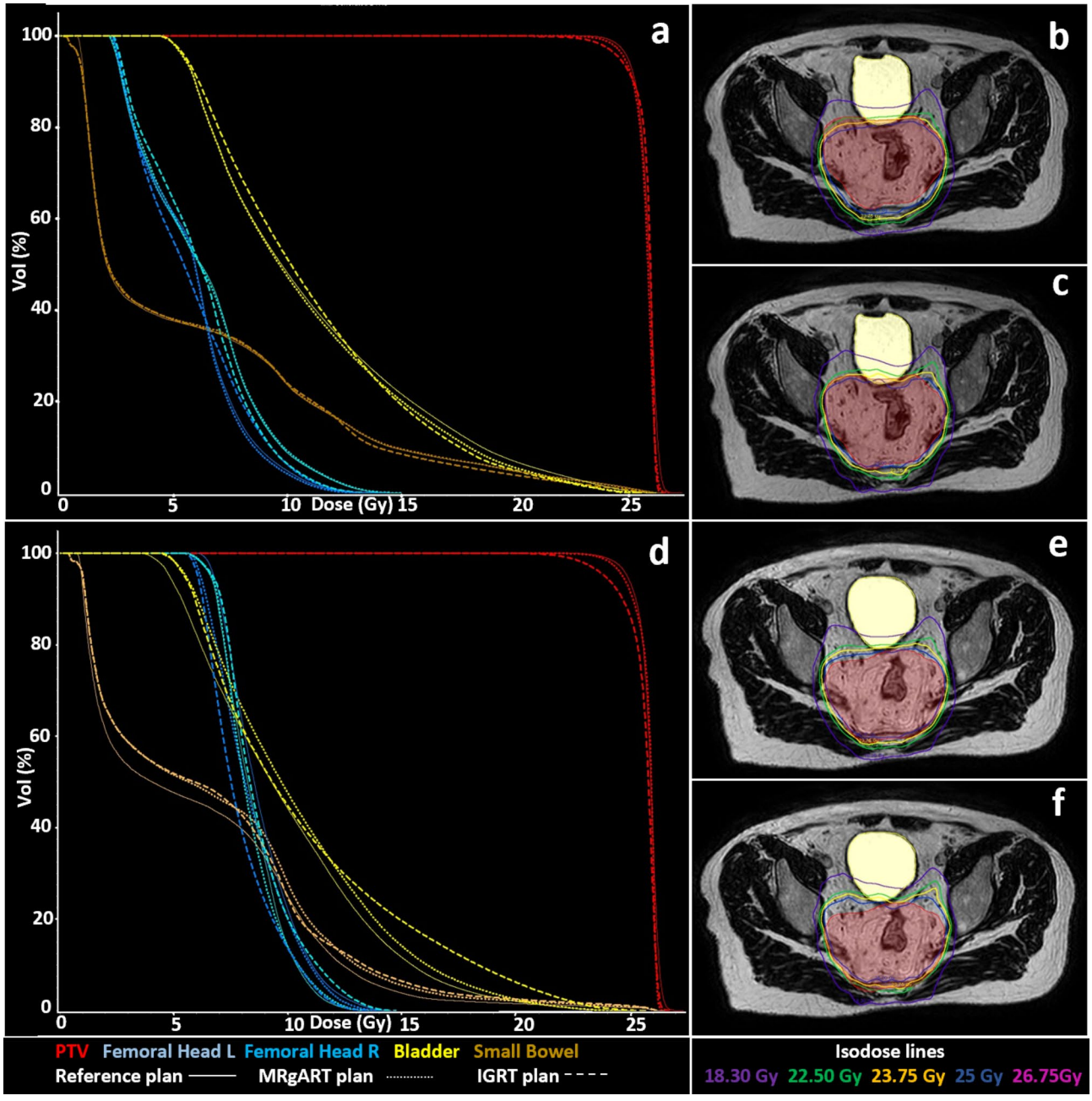

Fig. 2 Dose-volume histograms (DVHs) and isodoses distributions following dose accumulation on the first and last MRI images for a representative patient in IGRT and MRgART workflows. Image (**a**) and **d**) show the DVHs from the dose accumulation on the first and last fractions, respectively. Images (**b**) and **e**) show the dose distributions for the MRgART workflow, and images (**c**) and **f**) for the IGRT workflow, all resulting from dose accumulation on the first and last MRI, respectively

average decrease in $V_{23.75}$ was 2.78% (range, 1.65–4.16%), with 5 of these also having $V_{26.75}$ exceeding values. For the OARs, bladder D_{15cc} values obtained with TP_{adap} are very close to the threshold, with a median value of 18.18 Gy and 56 fractions out of 95 below the limit of 18.30 Gy. In comparison, the IGRT plan showed poorer results, with only 34 fractions below the limit and a median value of 19.60 Gy (range 15.07–24.37 Gy). For the small bowel in the adapted workflow, the constraints were respected for each adaptive fraction, while for the IGRT workflow, 21% of the fractions exceeded the limits.

The results from the dose accumulation process on the MRI imaging of both the initial and final fractions for the adaptive and IGRT workflows are shown in Table 3. The dose accumulation in the first and last fraction does not present statistical differences ($p>0.05$) in the adaptive workflow, whereas significant differences were found in the IGRT workflow. The dose accumulation in the

adaptive workflow confirms the results obtained with the single fractions, confirming the compliance between planned and delivered doses. In the IGRT workflow, with the dose accumulation process, target coverage is improved compared to the single fractions results, and the doses to the small bowel and bladder are lower. However, despite these improvements, the target coverage and OARs constraints were still not met for 10 out of 19 patients, for the accumulation on the first fraction and 12 out of 19 patients in the last fraction. Figure 2 shows for a representative patient the DVH of the doses accumulated on the first and last fraction for the IGRT and MRgART workflows.

Discussion

This study aimed to evaluate the effectiveness of MRgART versus conventional image-guided radiotherapy (IGRT) for rectal cancer patients undergoing a SCRT comparing the dosimetry of the single fractions and of the whole treatment by dose accumulation. Our results indicate significant differences in dosimetric outcomes between the single fractions delivered with MRgART and IGRT, with MRgART demonstrating the capability to maintain planned dose distribution and respect OARs constraints. Previous studies have highlighted the advantages of MRgART for other tumor sites in improving target coverage and reducing OAR exposure [26, 27] by providing superior soft tissue contrast and enabling daily plan adjustments; our findings specific for rectum SCRT treatments align with these studies, while the assessment on corresponding simulated IGRT plans on the single fractions showed its use cannot ensure dosimetric reliability.

The advantages of an MRgART workflow [7, 8, 14] and uncertainties in the dose accumulation process [16, 17, 28, 29] have been deeply investigated, nevertheless, no specific studies regarding the rectum SCRT treatment were found. Dose accumulation was conducted using both MRgART and IGRT workflows and the accumulation process was carried out by projecting the dose back onto the anatomy of the first fraction and forward onto the anatomy of the last fraction, allowing a comprehensive comparison. This approach confirmed the accuracy of the adaptive workflow in satisfying all clinical criteria for the whole patient cohort, even reducing the target volume receiving 26.75 Gy. The accumulation process yielded improved results for the patients in the IGRT workflow, decreasing dosimetric discrepancies in target coverage. Particularly it improves adherence to the high-dose constraint (V26.75 < 15 cc) by dispersing small dose hot spots which were randomly located in the single fractions, thereby mitigating overdosage. Despite these improvements, more than half of the patients still did not meet the clinical requirements. Doses accumulated post-radiotherapy serve to determine whether the goals of the treatment were met, for individual dose assessment, but may also support the analysis of side effects and treatment response by reliable dosimetry.

This research presents inherent limitations. The retrospective nature of the study and the relatively small sample size of 19 patients may limit the generalizability of the findings. Variability in the quality of MR images obtained during treatment, due to differences in MRI protocols can affect image readability and consequently reduce the accuracy of adapted plans. Regarding the dose accumulation, the DIR may lead to large uncertainties in the registration and mapped dose, particularly in regions where high dose gradients are present [29]; in the case of our study at the edge between the bladder and target. Additionally, the study focused on a specific treatment regimen (25 Gy in 5 fractions) for rectal cancer. While this regimen is standard for SCRT, the findings may not be directly applicable to other dose schedules or tumors sites.

Despite these limitations, future researches may prioritize larger, prospective studies to validate these findings and investigate the broader applicability of MRgART across various cancer types and treatment protocols. Emphasis should be placed on the targeted use of dose accumulation for specific workflows, treatment protocols, and treatment sites. Additionally, the use of biologically corrected doses for dose accumulation could offer valuable insights into the true correlation between delivered doses and treatment outcomes.

Conclusion

MRgART for rectal cancer treatments in a short course of radiotherapy ensures that the delivered dose accurately matches the planned dose for each fraction. In contrast, IGRT may result in target coverage discrepancies and non-compliance with bladder and small bowel constraints. While the dose accumulation procedure did not highlight significant differences from the single fractions in the MRgART workflow, it may be considered if the IGRT workflow is followed.

Abbreviations

CRC	Colon rectal cancer
TME	Total mesorectal excision
SCRT	A short course of radiotherapy
MRI	Magnetic resonance imaging
CT	Computed tomography
OARs	Organs at risk
IGRT	Image-guided radiotherapy
PTV	Planning target volume
MR-Linacs	Magnetic resonance linear accelerators
MRgART	Magnetic resonance-guided adaptive radiotherapy
DVH	Dose-volume histogram
sCT	Synthetic CT
ED	Electron density.
TP_{IGRT}	Treatment plan of the IGRT workflow
TP_{adap}	Treatment plan of the adaptive workflow

Acknowledgements
None.

Author contributions
Authors contribution: Design of the Research: XX, TB, LCO; Images analysis and data processing: LJY, WF, LM; XX; LCO; Statistical analysis: LXF, LJ, Manuscript Preparation: ML, YF, WX, XX, TB; Writing Manuscript LCO, QZ, TB. All authors read and approved the final manuscript.

Funding
Sichuan Cadres health and fitness research project, ZH2023-801; Sichuan Province Science and Technology Program, 2023YFWZ0004.

Data availability
No datasets were generated or analysed during the current study.

Declarations

Ethics approval and consent to participate
The authors declare that this retrospective study "Dose tracking assessment for Magnetic Resonance Guided Adaptive Radiotherapy of rectal cancers" received the approval of the ethics Committee of Sichuan Cancer Hospital located in 55th Renmin South Road, 4th Section, 610041, Chengdu, China (Approval number SCCHEC-02-2021-026).

Consent for publication
Even if no individual patient data were reported, consensus has been received by every patient for the elaboration of its data and a future scientific publication.

Competing interests
The authors declare no competing interests.

Author details
[1] College of Nuclear Technology and Automation Engineering, Chengdu University of Technology, No.1 East 3 road ErXian bridge, Chengdu, China
[2]Department of Radiation Oncology, Sichuan Cancer Hospital & Institute, Radiation Oncology Key Laboratory of Sichuan Province, Affiliated Cancer Hospital of University of Electronic Science and Technology of China, No.55, the 4th Section, Chengdu Renmin South Road, Chengdu, China

Received: 19 July 2024 / Accepted: 17 August 2024
Published online: 02 September 2024

References

1. Rebecca L, Siegel ANG, Ahmedin J. Cancer Statistic 2024. CA: A Cancer Journal for Clinicians 2024;74(1):12–49.
2. Zheng R, Chen R, Han B, Wang S, Li L, Sun K et al. Cancer incidence and mortality in China, 2022. Zhonghua Zhong Liu Za Zhi (All-China Federation of Trade Unions) 2024;46(3):221–31.
3. Bong Hyeon K, Hyeon Min C. Overview of Radiation Therapy for treating rectal Cancer. Annals Coloproctology. 2014;30(4):165–74.
4. van de Velde CJ BP, Borras JM, Coebergh JW, Cervantes A, Blomqvist L. EURECCA colorectal: multidisciplinary management: European consensus conference colon & rectum. Eur J Cancer. 2014;50(1):e11–134.
5. Bahadoer R, Dijkstra E, Etten BV, Marijnen C, Putter H, Kranenbarg E et al. Short-course radiotherapy followed by chemotherapy before total mesorectal excision (TME) versus preoperative chemoradiotherapy, TME, and optional adjuvant chemotherapy in locally advanced rectal cancer (RAPIDO): a randomised, open-label, phase 3 trial. Lancet Oncol. 2020.
6. Van Gijn W, Marijnen CA, Nagtegaal BID, Kranenbarg A, Meershoek, Klein, Putter AH, Wiggers CT, et al. Preoperative radiotherapy combined with total mesorectal excision for resectable rectal cancer: 12-year follow-up of the multicentre, randomised controlled TME trial. Lancet Oncol. 2011;12(6):575–82.
7. Chiloiro G, Gani C, Boldrini L. Rectal Cancer MRI guided Radiotherapy: a practical review for the physician. Semin Radiat Oncol. 2024;34(1):64–8.
8. Boldrini L, Intven M, Bassetti M, Valentini V, Gani C. MR-Guided radiotherapy for rectal Cancer: current perspective on Organ Preservation. Front Oncol. 2021;11:619852.
9. Kondor AE, Baracs J, Imre M, Faluhelyi N, Bogner B, Hegedűs I et al. The role of MRI in the indication of the neoadjuvant chemo-radiotherapy for rectal cancer. Eur J Surg Oncol. 2019;45(2).
10. Feng X, Tang B, Wang P, Kang S, Liao X, Yao X, et al. Effectiveness of bladder filling control during online MR-Guided adaptive Radiotherapy for Rectum Cancer. Int J Radiat Oncol Biol Phys. 2023;117(2):e725–26.
11. Wang C, Wang Z, Min M, Yu X, Dong J, Wen B. The application of image guided Radiotherapy on the Precision of Intensity Modulated Radiotherapy in patients with locally advanced rectal Cancer. 医学物理学、临床工程、放射肿瘤学(英文). 2018;7(4):12.
12. Shortall JVO, E.Cree A, Dubec M, Kirkby A, Mackay K, van Herk R. M. Inter- and intra-fractional stability of rectal gas in pelvic cancer patients during MRIgRT. Med Phys. 2021;48(1).
13. ICRU Report 97. MRI-Guided radiation therapy using MRI-Linear accelerators. J ICRU. 2022;22(1):1–100.
14. Intven M, Otterloo S, Mook S, Doornaert P, De Groot-va Breugel E, GG S, et al. Online adaptive MR-guided radiotherapy for rectal cancer; feasibility of the workflow on a 1.5T MR-linac; clinical implementation and initial experience. Radiother Oncol. 2021;154:172–78.
15. Kensen CM, Janssen TM, Betgen A, Wiersema L, Peters FP, Remeijer P, et al. Effect of intrafraction adaptation on PTV margins for MRI guided online adaptive radiotherapy for rectal cancer. Radiation Oncol (London England). 2022;17(1):110.
16. McDonald BA, Zachiu C, Christodouleas J, Naser MA, Ruschin M, Sonke JJ, et al. Dose accumulation for MR-guided adaptive radiotherapy: from practical considerations to state-of-the-art clinical implementation. Front Oncol. 2022;12:1086258.
17. Regnery S, Leiner L, Buchele C, Hoegen P, Sandrini E, Held T, et al. Comparison of different dose accumulation strategies to estimate organ doses after stereotactic magnetic resonance-guided adaptive radiotherapy. Radiat Oncol. 2023;18(1):92.
18. Stereotactic Ablative Body Radiation Therapy (SABR). A Resource. The faculty of clinical Oncology of the Royal College of radiologists. 2019.
19. Pollom EL, Chin AL, Diehn M, Loo BW, Chang DT. Normal tissue constraints for abdominal and thoracic stereotactic body Radiotherapy. Semin Radiat Oncol. 2017;27(3):197–208.
20. Benedict S, Yenice K, Followill D, Galvin J, Hinson W, Kavanagh B, et al. Stereotactic body radiation therapy: the report of AAPM Task Group 101. Med Phys. 2010;37(8):4078–101.
21. Appelt AL, Kerkhof EM, Nyvang L, Harderwijk EC, Marijnen C. Robust dose planning objectives for mesorectal radiotherapy of early stage rectal cancer – a multicentre dose planning study. Tech Innovations Patient Support Radiation Oncol. 2019;11:14–21.
22. Hanna GG, Murray L, Patel R, Jain S, Aitken KL, Franks KN, et al. UK Consensus on normal tissue dose constraints for stereotactic Radiotherapy. Clin Oncol (R Coll Radiol). 2018;30(1):5–14.
23. Wang C, Chao M, Lee L, Xing L. MRI-based treatment planning with electron density information mapped from CT images: a preliminary study. Technol Cancer Res Treat. 2008;7(5):341.
24. Tang B, Liu M, Wang B, Diao P, Li J, Feng X, et al. Improving the clinical workflow of a MR-Linac by dosimetric evaluation of synthetic CT. Front Oncol. 2022;12:920443.
25. Chetty IJ, Rosu-Bubulac M. Deformable Registration for Dose Accumulation - ScienceDirect. Semin Radiat Oncol. 2019;29(3):198–208.
26. Menten MJ, Wetscherek A, Fast MF. MRI-guided lung SBRT: Present and future developments. Physica Med. 2017: S1120179717300327.
27. Ristau J, Hrner-Rieber J, Buchele C, Jkel SKlüter, Baumann C. Stereotactic MRI-guided radiation therapy for localized prostate cancer (SMILE): a prospective, multicentric phase-II-trial. Radiation Oncol (London England). 2022;17(1):75.
28. Lena N, Florian AM, Murr, Ben Archibald H, Marco F, Mohammad H, Wolfgang L, et al. Review and recommendations on deformable image registration uncertainties for radiotherapy applications. Phys Med Biol. 2023;68:24TR01.

29. Murr M, Brock KK, Fusella M, Hardcastle N, Hussein M, Jameson MG et al. Applicability and usage of dose mapping/accumulation in radiotherapy. Radiother Oncol. 2023;182.

Publisher's note